

LETTER • OPEN ACCESS

Changes in fire-season burned area in northeastern China regulated by tropical North Atlantic variability

To cite this article: Wenjian Hua *et al* 2024 *Environ. Res. Lett.* **19** 124086

View the [article online](#) for updates and enhancements.

You may also like

- [Social resilience to changes in climate over the past 5000 years](#)
Liang Emlyn Yang, Mara Weinelt, Ingmar Unkel *et al.*
- [Lack of evidence for alternative stable states in Northern Hemisphere forests during the past 8 ka](#)
Laura Schild, Raphaël Hébert, Ulrike Herzsuh *et al.*
- [Soil moisture–atmosphere coupling amplifies the change in extreme heat in inner East Asia under rapid summer warming](#)
Zejiang Yin, Buwen Dong, Song Yang *et al.*



The Electrochemical Society
Advancing solid state & electrochemical science & technology

UNITED THROUGH SCIENCE & TECHNOLOGY

248th ECS Meeting Chicago, IL October 12-16, 2025 *Hilton Chicago*



Science + Technology + YOU!

SUBMIT ABSTRACTS by March 28, 2025

SUBMIT NOW

ENVIRONMENTAL RESEARCH
LETTERS

LETTER

OPEN ACCESS

RECEIVED
4 June 2024REVISED
30 October 2024ACCEPTED FOR PUBLICATION
21 November 2024PUBLISHED
29 November 2024

Original content from
this work may be used
under the terms of the
[Creative Commons
Attribution 4.0 licence](#).

Any further distribution
of this work must
maintain attribution to
the author(s) and the title
of the work, journal
citation and DOI.

Changes in fire-season burned area in northeastern China
regulated by tropical North Atlantic variabilityWenjian Hua^{1,*} , Lu Zhou¹ , Yan Jiang² , Liming Zhou³ , Xiyan Xu⁴ and Haishan Chen^{1,*}

¹ Key Laboratory of Meteorological Disaster, Ministry of Education/Joint International Research Laboratory of Climate and Environment Change/Collaborative Innovation Center on Forecast and Evaluation of Meteorological Disasters, Nanjing University of Information Science and Technology, Nanjing, People's Republic of China

² School of Global Policy and Strategy, University of California, San Diego, La Jolla, CA, United States of America

³ Department of Atmospheric and Environmental Sciences, University at Albany, State University of New York, Albany, NY, United States of America

⁴ Key Laboratory of Regional Climate–Environment for Temperate East Asia, Institute of Atmospheric Physics, Chinese Academy of Sciences, Beijing, People's Republic of China

* Authors to whom any correspondence should be addressed.

E-mail: wenjian@nuist.edu.cn and haishan@nuist.edu.cn

Keywords: burned area, northeastern China, fire weather conditions, tropical North Atlantic

Supplementary material for this article is available [online](#)

Abstract

Mapping and monitoring regional fire activity are essential to understand their responses to human activities and climate change. Here we use multiple sources of observations, reanalysis data, and model simulations to examine the responses of fire activity to climate change over northeastern China in the past two decades. We detected significant positive burned area (BA) trends in this region since 2003 during spring and much stronger interannual variations in BA in the last decade. We then separated the study region into cropland and natural vegetation and found that the increasing BA trends come mainly from agricultural burning. Our results also show that temperature is the dominant driver for BA variations in natural vegetation, whereas agricultural burning is influenced by precipitation, although human activities largely contribute to BA variations due to farming practices and land use and management. Our results further suggest that tropical North Atlantic (TNA) sea surface temperatures (SST) variability regulates the fire weather conditions (temperature and precipitation) in northeastern China through the Rossby wave train from the tropical Atlantic to the Eurasian continent. The cooling of TNA SST since 2010 could induce an anomalous anticyclonic circulation around Northeast Asia, leading to sinking motion and divergence in the region and resulting in reduced precipitation and warm temperatures. Thus, the co-occurrence of warm and dry anomalies has led to more frequent burning since the 2010s. Our study not only detects recent BA variations in northeastern China but also provides further evidence for the remote impact of TNA variability on recent BA and climate variations over the region.

1. Introduction

Fire is a natural process and a fundamental component of ecosystems (Bond *et al* 2005). Human activities and climate change have profound impacts on ecosystems, leading to changes in behaviors and impacts of fires (Jones *et al* 2022, 2024). For example, fire seasons are lengthening globally, and fire weather conditions are becoming more extreme in recent decades (Jolly *et al* 2015). In a warmer climate, fire potential

is projected to enhance across most burnable global land surfaces (Abatzoglou *et al* 2019). Hence, understanding the nature and cause of regional burning and assessing the fire–human–climate interactions are of significant socio-economic, ecological and environmental importance.

Fire activity is strongly influenced by weather conditions, human activities, fuels and ignition agents (Flannigan *et al* 2009). In general, variations in temperature, precipitation, relative humidity, and wind

speed have been proved to be the main meteorological drivers of fire activity (Jolly *et al* 2015, Jain *et al* 2022). Previous studies have suggested that temperature is a dominant factor controlling fires (Westerling *et al* 2006, Jain *et al* 2022), with warmer temperatures leading to more fires (Descals *et al* 2022, Senande-Rivera *et al* 2022). The linkages between precipitation and fire are more complex (Williams and Abatzoglou 2016), as precipitation can not only suppress fire potential by reducing flammability, but also promote the growth of surface fuels in fuel-limited fire regimes (Abatzoglou *et al* 2018, Holden *et al* 2018). Many studies have also explored the relationship between sea surface temperatures (SSTs) and fire activity for specific land regions at seasonal to multidecadal timescales (Chen *et al* 2011, Chen *et al* 2017b, Fang *et al* 2021, Cardil *et al* 2023). For example, the anomalous North Atlantic SSTs could enhance fire activity in the western Amazon (Fernandes *et al* 2011), southeastern Siberia (Meng and Gong 2022), and northern Scandinavia (Drobyshev *et al* 2016). Large-scale SST patterns influence the variability of regional burned areas (BAs) through climate controls on fuel amounts, continuity and moisture content. Although fire can occur naturally without human intervention (Marlon *et al* 2008), human activities (e.g. land use and management, human-caused fire ignitions or climate change) play a major role in recent fire activity (Andela *et al* 2017, Balch *et al* 2017, Williams *et al* 2019, Turco *et al* 2023).

It is worth noting that the trends in regional fire activity and their possible mechanisms remain uncertain due to substantial variations amongst biomes, interaction of biomass and climate, and human influences (Bowman *et al* 2020). For example, Jones *et al* (2022) reported that the sign of observed and modeled fire trends varied in South and North America, Russia and northern China. Northeastern China has experienced increased fire activity and biomass burning over the past decade (Chen *et al* 2017a, Yi *et al* 2017). Previous studies have suggested that the observed burning in northeastern China is influenced by human activities through fire ignition, spread and extinguishment (Zhang *et al* 2016, Zhuang *et al* 2018, Cui *et al* 2021, Lian *et al* 2023). Recent research showed that internal variability (e.g. El Niño-Southern Oscillation and sea ice) has also contributed to recent climate variations and fire activity in northeastern China (Fang *et al* 2021, Liu *et al* 2023). Cardil *et al* (2023) indicated that tropical North Atlantic (TNA) variability is the leading climate teleconnection mode related to BA and is responsible for regulating fire weather conditions, particularly in the Northern Hemisphere. However, a comprehensive and quantitative assessment of the TNA's influence on burning in northeastern China and its role in observed fire activity are largely unknown. It is thus imperative to investigate

the potential links between TNA SST and fire weather conditions and fire activity in this region.

In this study, we first use satellite data to examine the potential responses of fire activity to climate change over northeastern China in the past two decades and then quantify the contributions of climatic effects to regional burning. We further investigate how the TNA SST forcing influences the fire weather conditions associated with fire activity in this region. Our results could enhance our understanding of how fire activity may change in a warming climate and could be critical for adaptation and disaster risk management.

2. Data and methods

2.1. Observational, reanalysis and coupled model data

We analyzed the BA products from the moderate resolution imaging spectroradiometer (MODIS), European Space Agency (ESA), and global fire emissions database (GFED). The primary BA data set used in this study is the monthly, gridded 500 m product from the Terra and Aqua combined MCD64A1 version 6.1 during 2001–2022 (Giglio *et al* 2018). The MCD64A1 burned-area mapping approach employs 500 m MODIS imagery coupled with 1 km MODIS active fire observations. We also used the BA products from the ESA Climate Change Initiative version 5.1 (FireCCI51) (Lizundia-Loiola *et al* 2020) and the fourth version of the GFED4s grid (van der Werf *et al* 2017). The results of FireCCI51 and GFED4s are qualitatively similar to those of MODIS and thus are not shown separately in the main text. We also used the MODIS version 6.1 land cover product (MCD12C1) to identify the changes in vegetation type and percentage vegetation cover.

We used the monthly, gridded meteorological data (referred to CN05.1) from China Meteorological Administration on a 0.25° grid from 1961 to 2022. It was based on observations from more than 2400 surface meteorological stations over China (Wu and Gao 2013). Variables used in this study include daily mean, maximum (T_{\max}) and minimum (T_{\min}) temperatures, precipitation, relative humidity, and wind speed. We also analyzed the geopotential height, wind fields, surface shortwave radiation, and cloud cover data from the ECMWF Reanalysis v5 (ERA5) (Hersbach *et al* 2020) and the SST data from the Extended Reconstructed SST version 5 (ERSSTv5, Huang *et al* 2017). We used daily minimum relative humidity (RH_{min}), which was estimated using the vapor pressure equations (Allen *et al* 1998), to represent the fire weather condition of humidity.

As the major factors controlling fire activity, weather conditions could be remotely driven by SST variability, which modulates fire activity by indirectly regulating local/regional meteorological conditions via teleconnection. To investigate the impact

of North Atlantic SST variations on the fire weather conditions, we used the idealized Atlantic pacemaker experiments by the Phase 6 of the Coupled Model Intercomparison Project (CMIP6) models participating in the decadal climate prediction project (Boer *et al* 2016). We analyzed the pacemaker experiments by the Institute Pierre–Simon Laplace (IPSL) coupled climate model (i.e. IPSL-CM6A-LR). In the pacemaker experiments, SSTs are restored to model climatology plus a 12 month running mean of SST anomalies over the specific ocean regions (e.g. the TNA). Outside the restored region the model evolves freely allowing full climate system response. In this way, we can examine the impact of North Atlantic SST on the fire weather conditions around northeastern China.

2.2. Analysis methods

We focus on the period from 2003 to 2022, as the MODIS data may underestimate the BA pixels before around 2002 due to the availability of a single satellite (Terra) (Lizundia-Loiola *et al* 2020). We calculated the linear trends in BA using the Theil–Sen slope estimator, which is relatively insensitive to outliers. The significance of the Theil–Sen slope was estimated based on the Mann–Kendall test. To quantify the mean and trend in BA fraction, we first summed the raw data to a resolution of 0.25° . The BA fraction for each grid cell was calculated as the ratio between the number of pixels classified as ‘burned’ and the total number of valid pixels within the same cell. We then summed monthly data to seasonal BA. Finally, we calculated the mean and changes of BA in each grid box during 2003–2022.

Note that northeastern China is mostly covered by agricultural land and forests. We also examined the BA variations across land cover types. We separated our study region into two groups (i.e. cropland and natural vegetation) using MCD12C1 data. We defined the cropland as agricultural land and other land cover types as natural vegetation (non-cropland vegetation). We then analyzed the BA variations in each of the aggregated classes to examine their relative contributions to fire activity.

Given the strong linkage between BA and climate change, we assume that the climatic effects on BA are primarily the result of variations in temperature, precipitation, RHmin, and wind speed (Flannigan *et al* 2009, Jones *et al* 2022). To examine the regional SST-induced changes in atmospheric circulation and fire weather conditions, we performed correlation and regression analyses to reveal any coherent SST variations, and associated atmospheric circulation and climate changes. As TNA variability is the leading climate teleconnection mode related to BA and responsible for regulating the fire weather conditions in the Northern Hemisphere (Cardil *et al* 2023), we also analyzed the North Atlantic pacemaker experiments conducted by the IPSL-CM6A-LR model. Two 25-member ensembles of simulations were run for 10 yrs

and each simulation was specified with idealized SST (i.e. positive and negative SST anomalies in the TNA) configurations. We used the difference between the two experiments results to represent the TNA induced variations.

3. Results

3.1. Trends in BA

Most BAs in northeastern China occurred in the Songnen Plain (figure 1(a)). The western parts of Heilongjiang and Jilin provinces are at the center of the area burned (figures 1(a) and S1–S2). The burning usually happens in spring and autumn, associated with high temperatures and low precipitation (figure S3). We found significant positive annual BA trends in northeastern China since 2003 and all the BA products demonstrated increasing trends and similar interannual variability (figure S4). We focus on the spring months (March, April and May, MAM) when the BA trend is the strongest in northeastern China.

Positive trends in spring BA occurred predominantly in the northwestern parts of Heilongjiang and central-western Jilin provinces during 2003–2022 (figure 1(b)). The BA is relatively smooth before the 2010s, but experiences significant interannual variations in the last decade, with larger magnitudes than the first decade (figure 1(e)). In general, MAM-mean BA records in northeastern China have almost sextupled from ~ 0.19 Mha before 2010 to over 1.2 Mha in 2022, with the strongest BA variations in the last decade. The regional-mean area burned has sharply increased from 2003 to 2022, by 0.05 Mha per year or by 0.07 Mha per year between the last and first decades for the period 2003–2022.

We then separated the study region into cropland and natural vegetation. We estimated that $\sim 78\%$ of total BA variations between 2003 and 2022 occurred in agriculture land, while the residual ($\sim 22\%$) was from natural vegetation (figure 2). BA records in cropland increased from 2003 to 2022, by 0.06 Mha per year (figure 2(a)). In contrast, the trends of area burned in natural vegetation are insignificant (figure 2(b)).

3.2. Climate drivers of regional burning

We show the corresponding trends in T_{\max} and precipitation during 2003–2022. T_{\max} increases but the trends are insignificant over the study region (figure 1(c)) due to the strong interannual variability (figure 1(e)). The regional mean MAM T_{\max} reaches the lowest levels in 2010 and then recovers steadily thereafter. Precipitation tends to increase but is insignificant (figure 1(d)). It increases steadily from 2003 to 2010, despite strong interannual variability, and exhibits a decline trend since then (figure 1(e)). It is worth noting that BA and temperature reach their lowest levels in 2010, while precipitation demonstrates its highest value for the year 2010 (figure 1(e)).

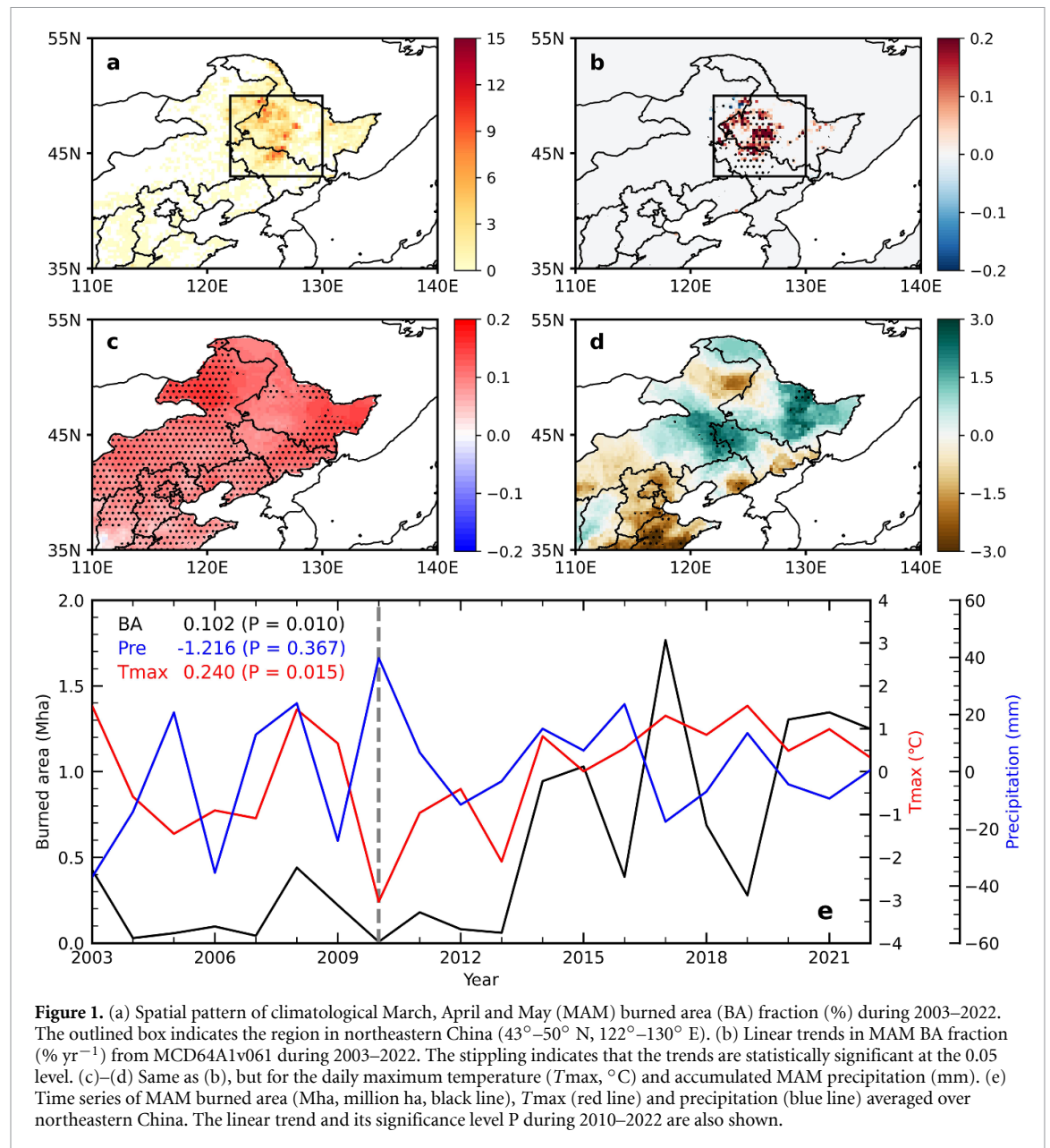


Figure 1. (a) Spatial pattern of climatological March, April and May (MAM) burned area (BA) fraction (%) during 2003–2022. The outlined box indicates the region in northeastern China (43°–50° N, 122°–130° E). (b) Linear trends in MAM BA fraction ($\% \text{ yr}^{-1}$) from MCD64A1v061 during 2003–2022. The stippling indicates that the trends are statistically significant at the 0.05 level. (c)–(d) Same as (b), but for the daily maximum temperature (T_{max} , $^{\circ}\text{C}$) and accumulated MAM precipitation (mm). (e) Time series of MAM burned area (Mha, million ha, black line), T_{max} (red line) and precipitation (blue line) averaged over northeastern China. The linear trend and its significance level P during 2010–2022 are also shown.

These results imply that the burning usually occurs at the intersection of hot weather and dry conditions.

Note that the BA in cropland is heavily influenced by human activities through fire ignition, spread, and extinguishment (Yi *et al* 2017), while the burning in natural vegetation is mainly associated with climate change. We further examine the connections between the BA in natural vegetation and climatic drivers. The fluctuations in BA in natural vegetation are in phase with the T_{max} variations ($r = 0.72$, $p < 0.01$) during 2003–2022 (figure 2(b)). We assess the relative importance of individual driving factors. T_{max} is identified as the dominant driver for regional BA and accounts for more than 40% of the variance (figure S5).

We also examine the correlation between the BA in cropland and climatic factors, although human

activities largely contribute to BA variations in cropland due to farming practices. We removed the trends estimated from linear regression, in order to highlight variability. It is worth noting that significant negative correlations are found between the BA and precipitation ($r = -0.40$, $p = 0.10$), indicating that precipitation is associated with BA in cropland. The linearly detrended BA in cropland and T_{max} are also correlated ($r = 0.35$, $p = 0.13$), although the association is not statistically significant. Our results suggest that the BA variations are accompanied by dry/wet conditions, as less (more) precipitation comes with larger (smaller) BA, in particular in the last decade (figure 2(a)).

To further support our analysis, we calculated and compared the linear trends for 2003–2010 and 2010–2022. These two periods are chosen because the

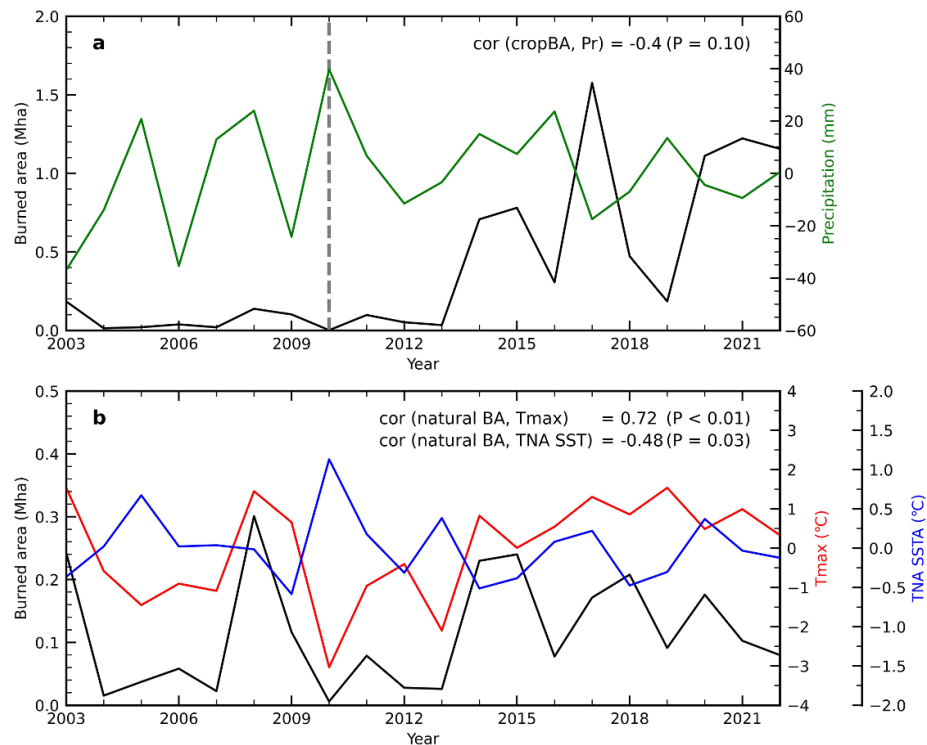


Figure 2. Time series of MAM burned area (Mha) averaged over the (a) agricultural land and (b) natural vegetation in northeastern China (43° – 50° N, 122° – 130° E). We used the MCD12C1 land cover data to separate the study region into two groups (cropland and natural vegetation) and analyzed the BA variations in each of the aggregated classes. Also shown in (a) are the correlation coefficient between BA in cropland and precipitation, together with the attained significance level (p). The correlation coefficients between BA in natural vegetation and T_{max} and TNA SST are also shown in (b). The TNA SST index was defined as the SST anomalies averaged over TNA (5.5° – 23.5° N, 15° – 57.5° W).

year 2010 is the time when the BA and temperature reached their lowest levels and then started an increasing trend, while precipitation peaked and then a declining trend started (figure 1(e)). The spatial patterns of linear trends for the weather conditions are shown in figure 3. The co-occurrence of hot temperatures, dry and windy conditions led to more frequent burning since the 2010s (figures 3(e)–(h)). In contrast, the weather conditions generally experienced the opposite variations before 2010, with colder temperature, more precipitation and less winds. We also analyzed soil moisture, which reflects fuel moisture conditions. Opposite trends are observed in the spatial patterns of soil moisture as well (figure S6). Our results demonstrate that the increasing BA trends, in particular in cropland, are associated with a shift towards favorable fire weather conditions.

3.3. TNA variability regulating the meteorological conditions

Regional climate variations are often attributed to changes in atmospheric circulations (Zhao and Liu 2019, Zhu *et al* 2021), which are remotely driven by the SST variability (Takaya *et al* 2021, Zhu *et al* 2023). The linkage between the T_{max} in northeastern China

and global SSTs reveals a tripolar pattern over the North Atlantic, with negative correlations in the tropical and subpolar regions and positive correlations in the subtropics (figure 4). For precipitation, significant positive correlations are observed in the TNA. Evidently, significant positive correlations are also seen between regional RHmin and TNA SST. That is, the large-scale coherence in correlations over TNA is compelling (figure 4). We also compared the linear trends for the first and last decades (figure S7). There also exist opposite trends in the spatial patterns of TNA SST. These results imply that the TNA SST is responsible for regulating the meteorological conditions around northeastern China.

To examine the relationship between TNA SST and fire weather conditions and BA, we defined the TNA index (TNAI) as the SST anomalies averaged over TNA (5.5° – 23.5° N, 15° – 57.5° W). We found that the BA variations in natural vegetation are significantly correlated with the TNA SST variability ($r = -0.48$, $p = 0.03$; figure 2(b)), suggesting the contribution of TNA SST variability to natural BA variations and weather conditions around northeastern China. Figure 5 shows the regression patterns of geopotential height, winds, precipitation, SST and T_{max} fields onto the TNAI index. It is noted that the

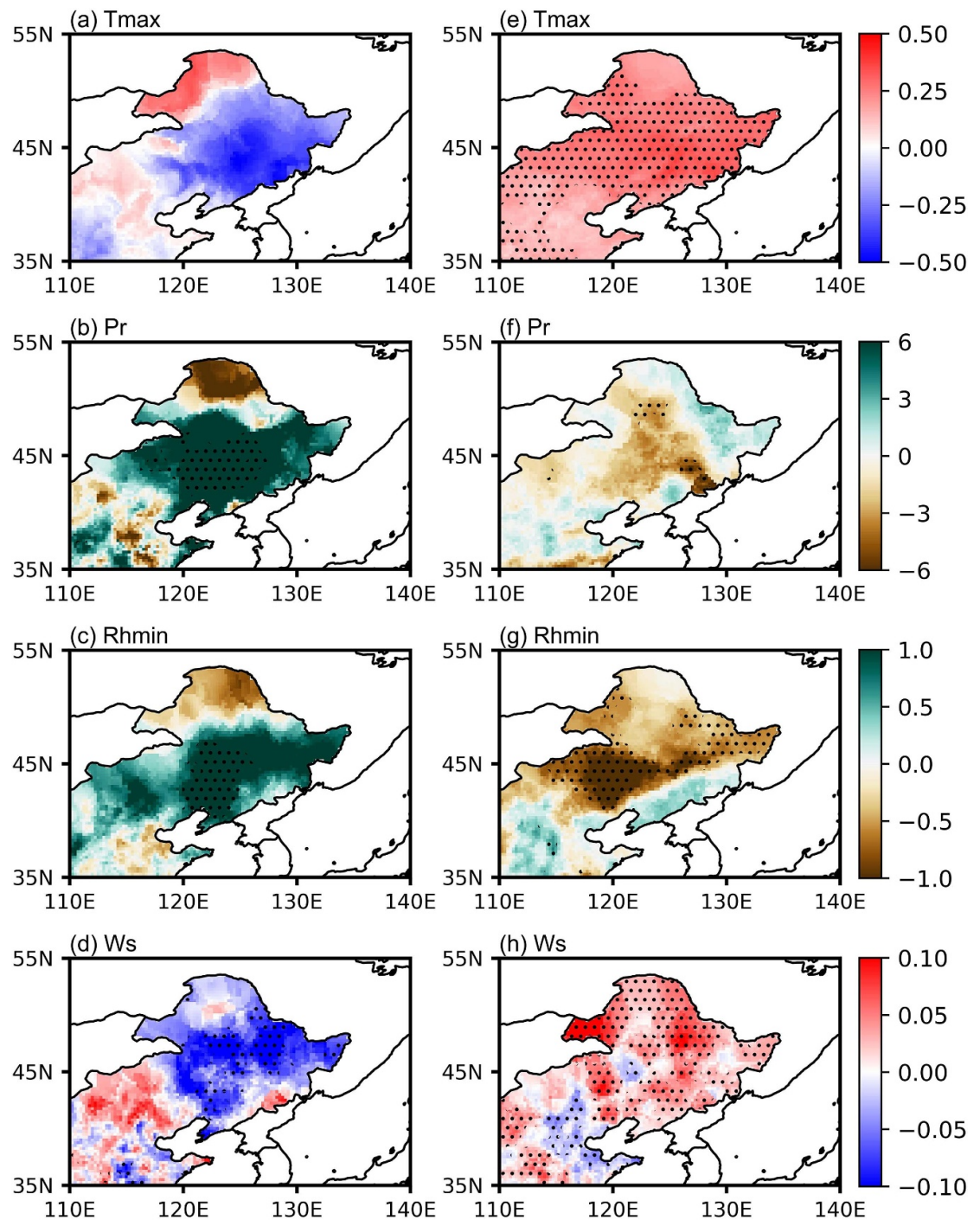


Figure 3. Linear trends during (a)–(d) 2003–2010 and (e)–(h) 2010–2022 in MAM daily maximum temperature (T_{\max} , $^{\circ}\text{C}$), precipitation (Pr , mm), daily minimum relative humidity (RH_{\min} , $\%$), and mean wind speed (Ws , m s^{-1}) from the CN05.1 data. The stippling indicates that the trends are statistically significant at the 0.1 level.

TNA SST forcing is accompanied by the Rossby wave train from tropical Atlantic to Eurasian continent. The Rossby wave train has five anomalous pressure centers and cyclonic/anticyclonic circulations around extratropical North Atlantic, southern Greenland, northern Europe, central Asia, and northeastern China, and exhibits equivalent barotropic structures (figure 5). The TNA cooling could induce an anomalous anticyclonic circulation around northeast Asia, leading to the divergence of moisture there. The

anomalous sinking and divergence result in less precipitation and warmer temperature. Furthermore, TNA cooling-related decreased cloudiness also leads to increased net surface solar radiation around northeast Asia (figure S8). Thus, the co-occurrence of warm and dry anomalies has led to more frequent burning since the 2010s.

To further this finding, we also examined the TNA induced atmospheric circulation changes in model simulations (figure 6). The cooling of TNA

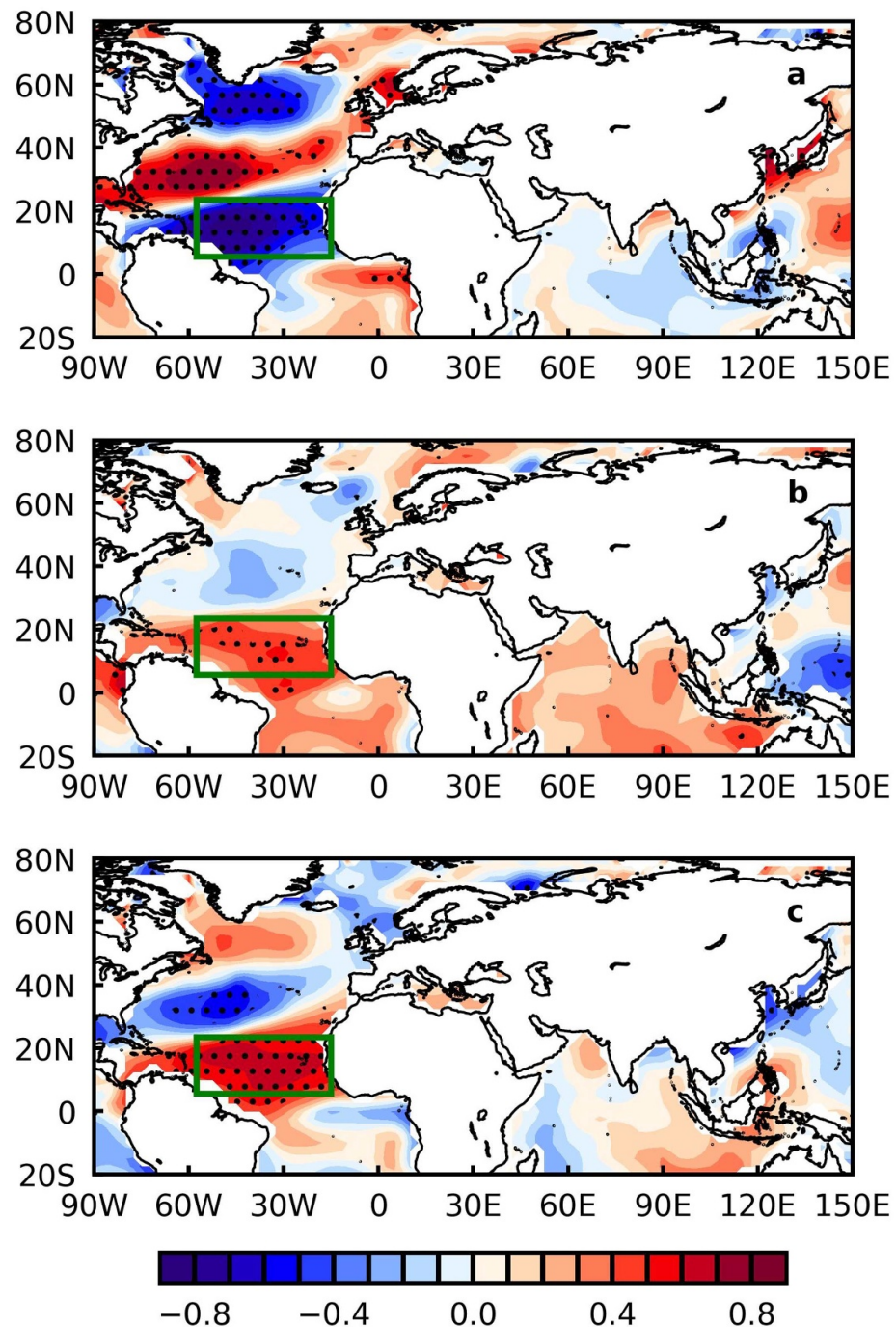


Figure 4. (a) Spatial patterns of correlation between T_{\max} averaged over northeastern China (black box in figure 1(a)) and local SSTs for the period 2003–2022. The stippling indicates that the correlations are statistically significant at the 0.05 level. The outlined green box indicates the region of tropical North Atlantic (5.5° N–23.5° N, 15° W–57.5° W). (b)–(c) Same as (a), but for (b) precipitation and (c) RHmin.

SST is associated with the northern Rossby wave train. The wave activity flux propagates northeastward from extratropical North Atlantic to northern Europe, central Asia, and then bends eastward to northeastern China (figure 6(a)). The anomalous anticyclonic anomaly pattern around East Asia could result in sinking motion and divergence there, leading to reduced precipitation and warm anomaly, although the temperature variations are relatively weak (figure 6(b)).

4. Discussion

We acknowledge the limitations and uncertainties in our study. First, most of the BA variations in northeastern China occur in cropland. The characteristics of BA are thus expected to be mainly influenced by human-caused fire ignitions (Yi *et al* 2017, Zhuang *et al* 2018). We also tested the BA variations by selecting the larger BAs over certain ranges of scale. In this way, we can filter out the smaller, prescribed fires

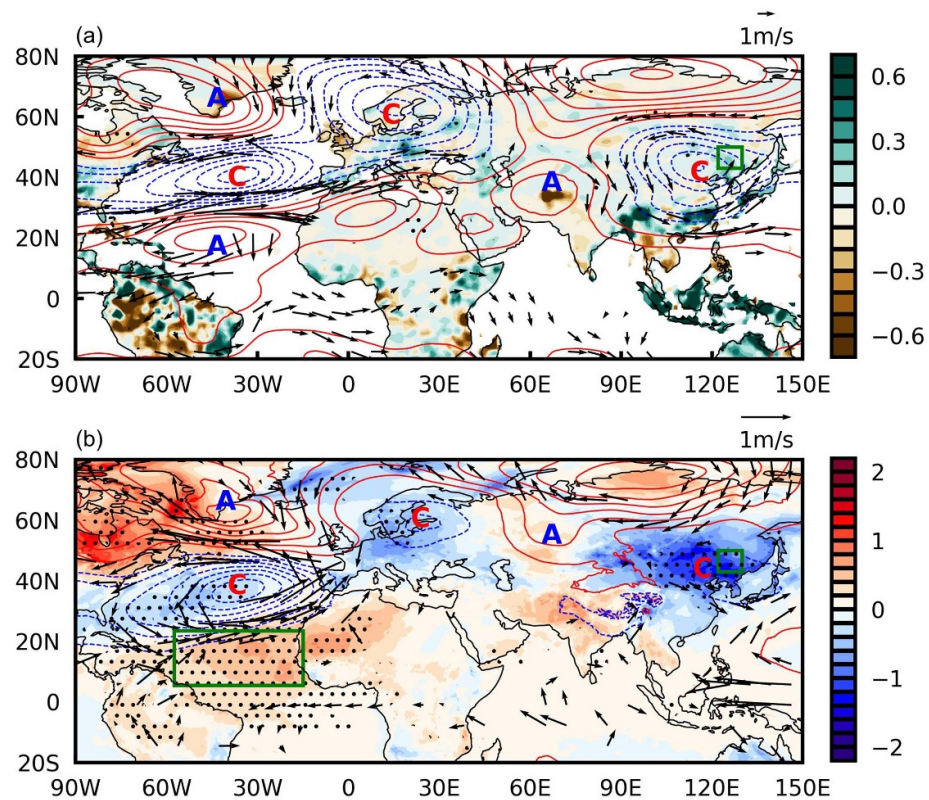


Figure 5. (a) Spatial regression patterns between the TNA SST index and 200 hPa horizontal winds (vectors, m s^{-1}) and geopotential height (contours, gpm), and precipitation (shading, mm/day). (b) Same as (a), but for the 850 hPa geopotential height (contours, gpm) and winds (vectors, m s^{-1}), SST and T_{max} (shading, $^{\circ}\text{C}$). The stippling indicates that the regression coefficients are statistically significant at the 0.05 level. The winds with black arrow are statistically significant at the 0.1 level. Letter A and C in (a) and (b) indicate the centers of anticyclonic/cyclonic anomalies.

due to human activities as more as possible. Results show that BA records also experience similar variations (figure S9). Please note that human activities, particularly in terms of ignition, are almost random and difficult to extract. And the relationships between climate and fire are generally modulated by non-climatic factors (e.g. human-caused fire ignitions), and likewise human drivers of fire often depend on the episodes of fire weather conditions. Hence, it is challenging to identify and quantify the climate-related or human-related BA variations where fires are both linked to climate change and human activities. One needs to interpret our results with these caveats in mind.

Second, land use and management also influence the BAs and introduce uncertainties in the estimated BA variations. The cropland fraction averaged over northeastern China generally shows an increasing tendency since 2003 (figure S10). It is thus reasonable to attribute the increasing trend in BAs to more and more crop residuals associated with the rising crop production in this region. We further examine the BA variations over the regions that have no land use change during 2003–2022 and compared the BA trends in agricultural land for both no land use change and land use change conditions. We estimate

that 12% of the agricultural burning is influenced by land use and management.

Third, the strict fire control policy could also limit the agricultural burning over the region (Chen *et al* 2017a, Cheng *et al* 2022). For instance, the fire suppression policy contributes to the decreasing fire occurrences after 2007 in eastern China (Fang *et al* 2021). Previous studies have also shown that the local emissions of open straw burning decreased in 2019 may result from the more stringent ban policy applied in 2019 in the People's Government of Jilin (Du *et al* 2022).

Fourth, it is worth noting that the peak fire season occurs primarily in April in northeastern China. Fire activity on Ching Ming Holiday (e.g. human-induced ignition sources occur in April) is especially high in China (Fang *et al* 2021). However, there has been no clear increase in fire activity on Ching Ming holiday in northeastern China during the last few decades (figure S11). Furthermore, it should be also noted that we take no account of the effects of snow during spring in northeastern China because there are no remarkable changes in snow mass over the study region (figure S12).

Furthermore, our results show that the natural BA variations are significantly correlated with the TNA

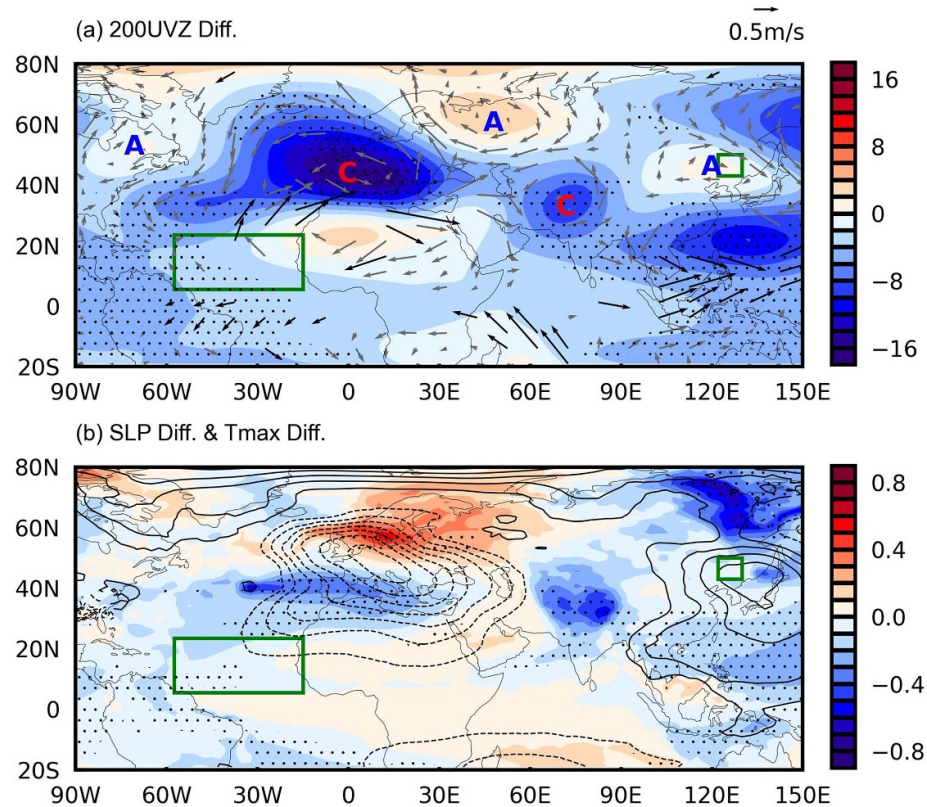


Figure 6. (a) The composite difference (negative minus positive SST anomalies) in 200 hPa horizontal winds (vectors, m s^{-1}) and geopotential height (contours, gpm). (b) Same as (a), but for the sea level pressure (contours, Pa) and Tmax (shading, $^{\circ}\text{C}$). The shading indicates that the regression coefficients are statistically significant at the 0.05 level. The winds with black arrow are statistically significant at the 0.1 level. Letter A and C in (a) indicate the centers of anticyclonic/cyclonic anomalies.

SST variability, suggesting the contribution of the North Atlantic SST variability to the BA variations and weather conditions over northeastern China (figure S13). Also, the linkage between the regional BA and SSTs reveals a tripolar pattern over the North Atlantic Ocean. The spatial pattern is similar to that of regional Tmax (figure 4(a)). These results imply that the North Atlantic tripole SST pattern also contributes to weather conditions (particularly Tmax) over northeastern China. We also examined the North Atlantic tripole SST pattern and the associated atmospheric circulation and climate changes. Results show that the tripole SST-related atmospheric circulation changes and fire weather conditions are relatively weaker (figure S14). Since the large-scale coherence in correlations for Tmax and precipitation is almost identical and compelling over TNA, we thus used the TNA as our key region in this study. On the interannual timescale, the North Atlantic SST tripole pattern and its influences are worthy of further investigation.

5. Summary

In this study, we show that BA experiences significant positive trends in northeastern China since 2003. BA records have almost sextupled from ~ 0.19 Mha

before 2010 to over 1.2 Mha in 2022, with the largest BA variations occurring in the last decade. We then separated the study region into cropland and natural vegetation and found that the increasing BA trends come mainly from agricultural burning. Our results further suggest that the BA variations in natural vegetation are primarily influenced by Tmax, which are remotely driven by North Atlantic SST variability. Observations and model simulations show that TNA SST is responsible for regulating the meteorological conditions in northeastern China. TNA SST forcing is accompanied by the Rossby wave train from tropical Atlantic to Eurasian continent. The TNA cooling since 2010 could induce an anomalous anticyclonic circulation around northeast Asia, leading to sinking motion and divergence there. Furthermore, our results also show that the fire weather conditions, in particular precipitation, contribute to the agricultural burning in the last decade. Whether the BA variations result from natural variability or human activities, climate change can influence and amplify the burning, particularly under hot, dry and windy conditions. Further efforts to assess the fire–human–climate interactions could help advance our understanding of fire activity and biomass burning over this region.

Data availability statement

The MCD64A1 data can be obtained from the Land Processes Distributed Active Archive Center website (<https://lpdaac.usgs.gov/products/mcd64a1v061/>). The FireCCI51 data can be obtained from <https://climate.esa.int/en/projects/fire/data/>. The GFED4s data can be obtained from www.globalfiredata.org/data.html. The CN05.1 data can be obtained from China Meteorological Administration (<http://data.cma.cn/en>). The MCD12C1 data can be obtained from <https://lpdaac.usgs.gov/products/mcd12c1v061/>.

All data that support the findings of this study are included within the article (and any supplementary files).

Acknowledgment

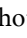
This work was supported by the National Key R&D Program of China (2022YFF0801601) and the National Natural Science Foundation of China (42075022). We acknowledge the High Performance Computing Platform of NUIST for their support of this work.

ORCID iDs

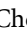
Wenjian Hua  <https://orcid.org/0000-0002-9705-3234>

Lu Zhou  <https://orcid.org/0009-0001-9701-6118>

Yan Jiang  <https://orcid.org/0000-0002-1472-2288>

Liming Zhou  <https://orcid.org/0000-0002-7009-2487>

Xiyan Xu  <https://orcid.org/0000-0003-2732-1325>

Haishan Chen  <https://orcid.org/0000-0002-2403-3187>

References

- Abatzoglou J T, Williams A P and Barbero R 2019 Global emergence of anthropogenic climate change in fire weather indices *Geophys. Res. Lett.* **46** 326–36
- Abatzoglou J T, Williams A P, Boschetti L, Zubkova M and Kolden C A 2018 Global patterns of interannual climate–fire relationships *Glob. Change Biol.* **24** 5164–75
- Allen R G, Pereira L S, Raes D and Smith M 1998 Crop evapotranspiration—guidelines for computing crop water requirements—FAO irrigation and drainage paper 56 (Food and Agriculture Organization of the United Nations, Rome)
- Andela N et al 2017 A human-driven decline in global burned area *Science* **356** 1356–62
- Balch J K, Bradley B A, Abatzoglou J T, Nagy R C, Fusco E J and Mahood A L 2017 Human-started wildfires expand the fire niche across the United States *Proc. Natl Acad. Sci. USA* **114** 2946–51
- Boer G J et al 2016 The decadal climate prediction project (DCPP) contribution to CMIP6 *Geosci. Model Dev.* **9** 3751–77
- Bond W J, Woodward F I and Midgley G F 2005 The global distribution of ecosystems in a world without fire *New Phytol.* **165** 525–38
- Bowman D M J S, Kolden C A, Abatzoglou J T, Johnston F H, van der Werf G R and Flannigan M 2020 Vegetation fires in the anthropocene *Nat. Rev. Earth Environ.* **1** 500–15
- Cardil A, Rodrigues M, Tapia M, Barbero R, Ramírez J, Stoof C R, Silva C A, Mohan M and De-miguel S 2023 Climate teleconnections modulate global burned area *Nat. Commun.* **14** 427
- Chen D, Pereira J M C, Masiero A and Pirotti F 2017a Mapping fire regimes in China using MODIS active fire and burned area data *Appl. Geogr.* **85** 14–26
- Chen Y, Morton D C, Andela N, van der Werf G R, Giglio L and Randerson J T 2017b A pan-tropical cascade of fire driven by El Niño/Southern Oscillation *Nat. Clim. Change* **7** 906–11
- Chen Y, Randerson J T, Morton D C, DeFries R S, Collatz G J, Kasibhatla P S, Giglio L, Jin Y and Marlier M E 2011 Forecasting fire season severity in South America using sea surface temperature anomalies *Science* **334** 787–91
- Cheng Y, Cao X-B, Liu J-M, Yu Q-Q, Zhong Y-J, Geng G-N, Zhang Q and He K-B 2022 New open burning policy reshaped the aerosol characteristics of agricultural fire episodes in Northeast China *Sci. Total Environ.* **810** 152272
- Cui S, Song Z, Zhang L, Shen Z, Hough R, Zhang Z, An L, Fu Q, Zhao Y and Jia Z 2021 Spatial and temporal variations of open straw burning based on fire spots in northeast China from 2013 to 2017 *Atmos. Environ.* **244** 117962
- Descals A, Gaveau D L A, Verger A, Sheil D, Naito D and Peñuelas J 2022 Unprecedented fire activity above the Arctic circle linked to rising temperatures *Science* **378** 532–7
- Drobyshev I, Bergeron Y, Vernal A D, Moberg A, Ali A A and Niklasson M 2016 Atlantic SSTs control regime shifts in forest fire activity of Northern Scandinavia *Sci. Rep.* **6** 22532
- Du Y, Zhao H, Zhang X and Xiu A 2022 Evaluation of the impacts of straw burning ban on air quality based on WRF-CMAQ *China Environ. Sci. (In Chinese with English Abstract)* **42** 5578–88 (available at: www.zghjcx.com.cn/CN/Y2022/V42/I12/5578)
- Fang K et al 2021 ENSO modulates wildfire activity in China *Nat. Commun.* **12** 1764
- Fernandes K et al 2011 North Tropical Atlantic influence on western Amazon fire season variability *Geophys. Res. Lett.* **38** L12701
- Flannigan M D, Krawchuk M A, de Groot W J, Wotton B M and Gowman L M 2009 Implications of changing climate for global wildland fire *Int. J. Wildland Fire* **18** 483–507
- Giglio L, Boschetti L, Roy D P, Humber M L and Justice C O 2018 The collection 6 MODIS burned area mapping algorithm and product *Remote Sens. Environ.* **217** 72–85
- Hersbach H et al 2020 The ERA5 global reanalysis *Q. J. R. Meteorol. Soc.* **146** 1999–2049
- Holden Z A, Swanson A, Luce C H, Jolly W M, Maneta M, Oyler J W, Warren D A, Parsons R and Affleck D 2018 Decreasing fire season precipitation increased recent western US forest wildfire activity *Proc. Natl Acad. Sci. USA* **115** E8349–E8357
- Huang B, Thorne P W, Banzon V F, Boyer T, Chepurin G, Lawrimore J H, Menne M J, Smith T M, Vose R S and Zhang H-M 2017 Extended reconstructed sea surface temperature version 5 (ERSSTv5), upgrades, validations, and intercomparisons *J. Clim.* **30** 8179–205
- Jain P, Castellanos-Acuna D, Coogan S C P, Abatzoglou J T and Flannigan M D 2022 Observed increases in extreme fire weather driven by atmospheric humidity and temperature *Nat. Clim. Change* **12** 63–70
- Jolly W M, Cochrane M A, Freeborn P H, Holden Z A, Brown T J, Williamson G J and Bowman D M J S 2015 Climate-induced variations in global wildfire danger from 1979 to 2013 *Nat. Commun.* **6** 7537
- Jones M W et al 2022 Global and regional trends and drivers of fire under climate change *Rev. Geophys.* **60** e2020RG000726
- Jones M W et al 2024 Global rise in forest fire emissions linked to climate change in the extratropics *Science* **386** eadl5889
- Lian C, Xiao C and Feng Z 2023 Spatiotemporal characteristics and regional variations of active fires in China since 2001 *Remote Sens.* **15** 54

- Liu G, Li J, Ying T, Su H, Huang X and Yu Y 2023 Increasing fire weather potential over Northeast China linked to declining Bering Sea ice *Geophys. Res. Lett.* **50** e2023GL105931
- Lizundia-Loiola J, Otón G, Ramo R and Chuvieco E 2020 A spatio-temporal active-fire clustering approach for global burned area mapping at 250 m from MODIS data *Remote Sens. Environ.* **236** 111493
- Marlon J R, Bartlein P J, Carcaillet C, Gavin D G, Harrison S P, Higuera P E, Joos F, Power M J and Prentice I C 2008 Climate and human influences on global biomass burning over the past two millennia *Nat. Geosci.* **1** 697–702
- Meng M and Gong D 2022 Winter North Atlantic SST as a precursor of spring Eurasian wildfire *Geophys. Res. Lett.* **49** e2022GL099920
- Senande-Rivera M, Insua-Costa D and Miguez-Macho G 2022 Spatial and temporal expansion of global wildland fire activity in response to climate change *Nat. Commun.* **13** 1208
- Takaya Y, Saito N, Ishikawa I and Maeda S 2021 Two tropical routes for the remote influence of the Northern Tropical Atlantic on the Indo–Western Pacific summer climate *J. Clim.* **34** 1619–34
- Turco M, Abatzoglou J T, Herrera S, Zhuang Y, Jerez S, Lucas D D, AghaKouchak A and Cvijanovic I 2023 Anthropogenic climate change impacts exacerbate summer forest fires in California *Proc. Natl Acad. Sci. USA* **120** e2213815120
- van der Werf G R et al 2017 Global fire emissions estimates during 1997–2016 *Earth Syst. Sci. Data* **9** 697–720
- Westerling A L, Hidalgo H G, Cayan D R and Swetnam T W 2006 Warming and earlier spring increase western U.S. forest wildfire activity *Science* **313** 940–3
- Williams A P and Abatzoglou J T 2016 Recent advances and remaining uncertainties in resolving past and future climate effects on global fire activity *Curr. Clim. Change Rep.* **2** 1–14
- Williams A P, Abatzoglou J T, Gershunov A, Guzman-Morales J, Bishop D A, Balch J K and Lettenmaier D P 2019 Observed impacts of anthropogenic climate change on wildfire in California *Earth's Future* **7** 892–910
- Wu J and Gao X 2013 A gridded daily observation dataset over China region and comparison with the other datasets *Chin. J. Geophys.* **56** 1102–11
- Yi K, Bao Y and Zhang J 2017 Spatial distribution and temporal variability of open fire in China *Int. J. Wildland Fire* **26** 122–35
- Zhang L, Liu Y and Hao L 2016 Contributions of open crop straw burning emissions to PM_{2.5} concentrations in China *Environ. Res. Lett.* **11** 014014
- Zhao F and Liu Y 2019 Atmospheric circulation patterns associated with wildfires in the monsoon regions of China *Geophys. Res. Lett.* **46** 4873–82
- Zhu X, Xu X and Jia G 2021 Asymmetrical trends of burned area between eastern and western Siberia regulated by atmospheric oscillation *Geophys. Res. Lett.* **48** e2021GL096095
- Zhu Z, Lu R, Fu S and Chen H 2023 Alternation of the atmospheric teleconnections associated with the Northeast China spring rainfall during a recent 60-years period *Adv. Atmos. Sci.* **40** 168–76
- Zhuang Y, Li R, Yang H, Chen D, Chen Z, Gao B and He B 2018 Understanding temporal and spatial distribution of crop residue burning in China from 2003 to 2017 using MODIS data *Remote Sens.* **10** 390